

Acoustically Driven Magnetized Target Fusion

M. Laberge, S. Howard, D. Richardson, A. Froese, V. Suponitsky, M. Reynolds, D. Plant
General Fusion Inc, Burnaby, BC, Canada (www.generalfusion.com)
Corresponding author e-mail: michael.delage@generalfusion.com.

Abstract— General Fusion is a 65-employee private company developing fusion energy with \$40M of capital to date. This report will describe General Fusion’s design for an acoustically driven Magnetized Target Fusion (MTF) reactor concept. The advantages of this particular MTF scheme will be discussed. Our experimental and numerical work and results so far will be presented, as well as plans for future development

Keywords—Magnetized Target Fusion;

I. INTRODUCTION

Magnetized Target Fusion (MTF) is a hybrid approach to fusion in which a self-organized plasma is compressed with the inertia of a conductive liner to conditions that fulfill the Lawson criterion [1]. Magnetized Target Fusion was first proposed in the 1970’s as a low-cost approach to fusion that combines the advantages of magnetic confinement fusion and inertial confinement fusion by working in an intermediate regime of plasma density and confinement time [2-4]. This paper provides an overview of the science behind MTF and the ongoing research at General Fusion to design, test, and demonstrate the ability to produce energy using its acoustic MTF technology. General Fusion is pursuing an acoustically-driven MTF concept that makes use of modern servo controllers which precisely synchronize piston impacts to create a large amplitude acoustic wave in the liquid metal liner. This wave will compress the target plasma in less than 200 μ s, similar to the practically achievable plasma lifetimes in modern self-organized plasma devices. An MTF reactor with the potential to achieve net gain can be developed given current technologies.

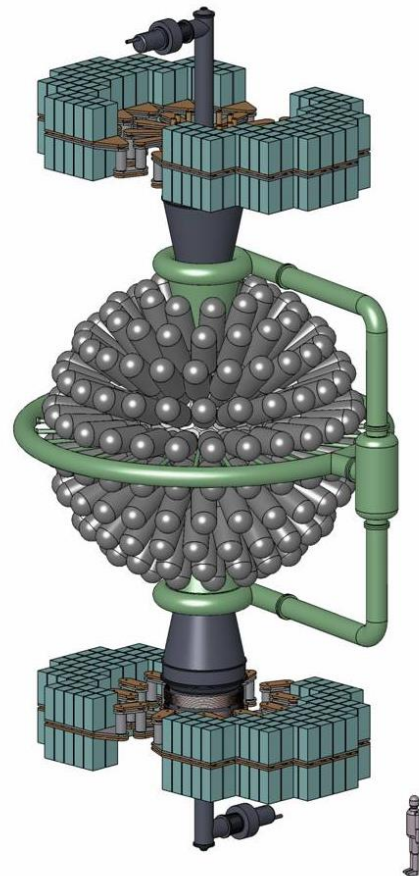
This paper summarizes General Fusion’s activities to prove the viability of its MTF technology. Efforts are focused on mitigating risks and testing full scale components for acoustically-driven compression of plasma in the proposed reactor, in order to validate the predicted plasma behavior and demonstrate net gain. The MTF program is divided into the following areas: Acoustics Driver, Plasma Injector, and in support of these, Numerical Simulation.

II. FUSION BY ACOUSTIC IMPLOSION

In General Fusion’s reactor design, the deuterium-tritium fuel is supplied as a pair of self-confined magnetized plasma rings, known as compact toroids (CT) that merge to form a single plasma ring within the compression region. This merging takes place as the pair of CTs are injected into the evacuated volume of a free-surface vortex in the center of a rotating flow of liquid metal. They merge in the center of this vortex cavity just prior to being compressed by the primary acoustic pressure wave. The optimal choice for the material of

this liquid metal, taking into account hydrodynamic and nuclear properties, is the molten form of the lead-lithium eutectic (atomic ratio 83% Pb, 17% Li, hereafter referred to as Pb-17Li). During the acoustically-driven implosion of the vortex free surface, the cavity volume is reduced by three orders of magnitude, raising the plasma density from 10^{22} ions/m³ to 10^{25} ions/m³, the temperature from 0.1 keV to 10 keV, and the magnetic field strength from 2 T to 200 T. The fusion energy will be generated during the 10 μ s that the plasma spends at maximum compression, after which the compressed plasma bubble causes the liquid metal wall to rebound. Most of the fusion energy is liberated as neutron radiation that directly heats the liquid metal. Using existing industrial liquid metal pumping technology the heated liquid metal is pumped out into a heat exchange system, thermally driving a turbine generator.

Fig. 1. General Fusion’s Acoustic MTF Reactor Concept.



The cooled liquid metal is pumped back into the vessel tangentially to reform the evacuated cylindrical vortex along the vertical axis of the sphere. Liquid Pb-17Li is ideal as a liner because it has a low melting point, low vapor pressure, breeds tritium, has a high mass for a long inertial dwell time, and has a good acoustic impedance match to steel, which equates to high efficiency in generating the acoustic pulse. The 100 MJ acoustic pulse is generated mechanically by a synchronized array of hundreds of pneumatically-driven pistons striking the outer surface of the reactor sphere. The acoustic pulse propagates radially inwards; geometric focusing results in an amplification of pressure from 1 GPa to 10 GPa at the liquid-plasma interface.

There are several practical advantages to designing an MTF implosion system around a pneumatic driver. First, pneumatic energy storage in the many 100 MJ range can be readily obtained at cost of less than \$0.2 per J, while the dominate alternative of high voltage pulsed power for electromagnetic implosion has proven to be significantly more expensive at greater than \$2/J. Additionally, for a practical reactor design, the same working gas (steam, CO₂ or He) on the high pressure end of the heat exchange system could be diverted to directly drive the piston array, eliminating any electrical losses involved in recharging and switching a massive capacitor bank.

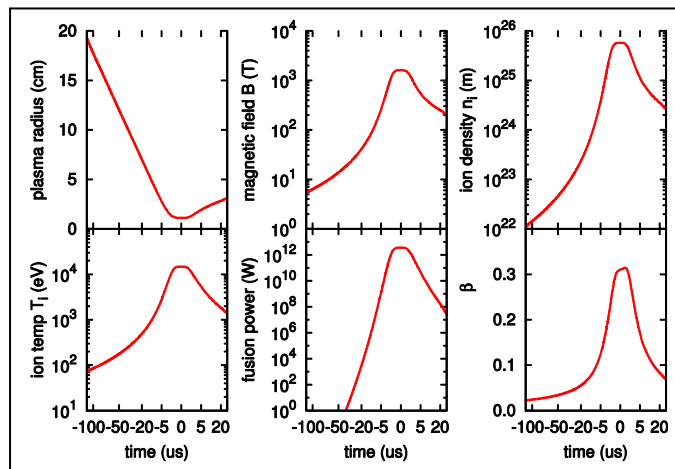
For a future power plant, economics, neutronics, tritium supply, and reactor energy density need to be considered. The eutectic absorbs the bulk of the fusion products through elastic scattering and provides a straightforward means of extracting the energy. The thick blanket significantly shields the wall by reducing the neutron flux on the structure and by lowering the neutron energy spectrum [5]. The 4π coverage provides an enhanced tritium breeding ratio of 1.6 to 1.8 [6]. The neutron multiplication factor results from the Pb(n,2n) reaction and also from the ${}^7\text{Li} + n \rightarrow {}^4\text{He} + {}^3\text{H} + n$ reaction as diagrammed by Moyer [7]. The challenge with a thick Pb-17Li liner is likely to be too much tritium production.

In order for the MTF compression to have significant fusion yield, the initial CT plasma needs to have sufficiently good magnetic confinement to survive the duration of the implosion, also high enough initial density and temperature that the final compressed state will exceed the Lawson criterion for the achievable compression ratio and dwell time. In addition the plasma energy confinement time needs to be sufficiently longer than the implosion time such that compressional heating can proceed in an approximately adiabatic fashion. The primary experimental-plasma campaign at General Fusion is focused on producing a self-confined target plasma with sufficient conditions that match our best estimates of these optimal pre-compression, fusion relevant parameters.

While efforts are underway to develop a fully 3D plasma-liner compression simulation that would accurately predict such goal parameters, there is still value in examining the result of more numerically tractable models to guide experimental operation and inform the design of longer range plans. Shown in Fig. 2 is the simulation of a spherically-

symmetric collapse using a 1D Lagrangian model of Pb liner coupled to point-plasma model. In this example scenario that gave near optimal fusion yield, a 2 GPa acoustic pulse is applied to the outer radius of the Pb at 1.5 m and takes 700 μs to propagate towards the plasma. At the plasma-liner interface, the pulse reaches 12 GPa and compresses the plasma in 130 μs . The plasma is 50-50 deuterium-tritium with an effective ion charge of 1.5. The plasma model includes the effects of adiabatic compression, Bremsstrahlung, Bohm thermal transport, fusion reaction chains, and fast alpha confinement. The time axis becomes more sparse around $t=0$ to better show the behavior during peak compression. The plasma is compressed radially by a factor of 18, increasing the magnetic field from 5 to 1600T, the ion density from 10^{22} to $6 \times 10^{25} \text{ m}^{-3}$, and the temperature from 0.1 to 15 keV. Peak fusion power is 3.6 TW and peak beta is 32%. The initial conditions for this compression scenario of $T_i = 100 \text{ eV}$, $n_i = 10^{22} \text{ m}^{-3}$, $\tau_E > 130 \mu\text{s}$ are within the range of achieved CT conditions, the one technically challenging parameter is $B_0 = 5 \text{ T}$, which is just beyond previous results yet not unreachable.

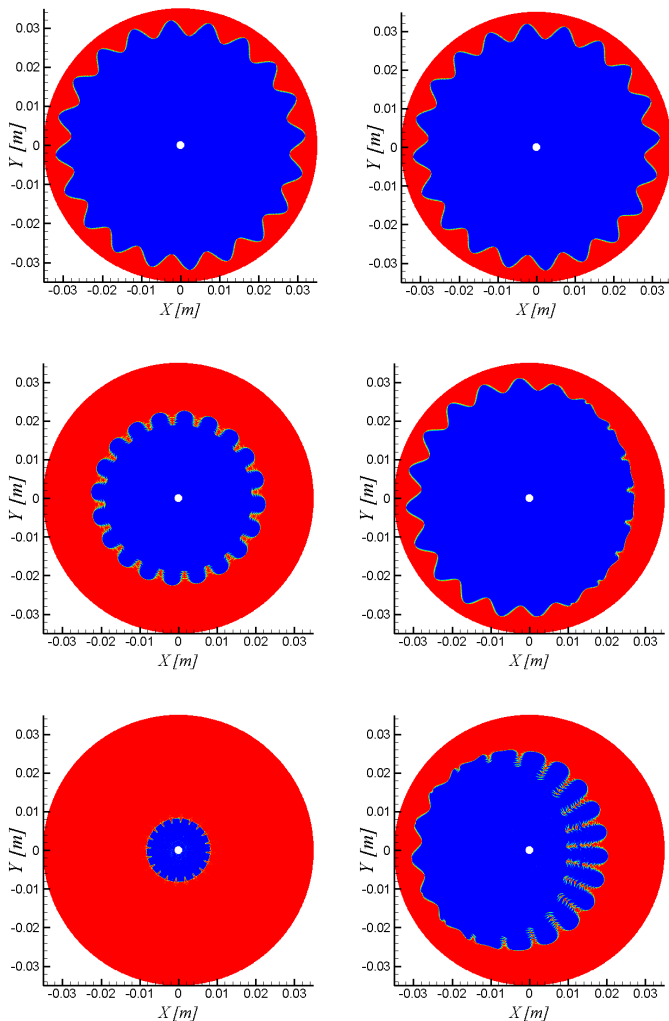
Fig. 2. Time-evolution of plasma parameters in a 1D Lagrangian model of Pb liner coupled to point-plasma model, showing Plasma-liner radius, CT magnetic field, ion density and temperature, fusion power, and plasma beta.



Yet another factor that enters into the design of the acoustically driven MTF reactor is the exact dynamics of the interaction between the focusing pressure wave and the free-surface of the vortex. This is intrinsically a multi-scale, 3D nonlinear system so it is challenging to simulate. At the largest scale the optimal configuration for the collapse of a CT would employ an imploding layer in the shape of an ellipsoid that encloses the CT with radially inward liner velocity. Yet the initial geometry of the vortex is that of a cylinder. To engineer such a dynamic transition between these geometries requires tailoring the shape of the pressure wavefront to accomplish pinching first above and below the CT before central compression occurs. CFD Simulations have shown that such a transition can be accomplished by sequencing the piston impacts with delays depending on vertical position to create an oblate ellipsoidal wave front.

A smaller-scale aspect of the wave-surface interaction dynamics is the onset of the Richtmyer-Meshkov (RM) instability, which in the worst possible case would completely undermine the ability of liner to cleanly compress the CT plasma. However to date all known analytic or computational studies of this instability are limited to planar or cylindrical interfaces. The ellipsoidal interface of the General Fusion compression scheme is outside of established methodology. Thus the ability to predict reliably a threshold for the acceptable level of initial perturbations (i.e. imperfection of the vortex surface, timing of the pistons, non-uniformity of Pb etc.) is an active area of research, and important for determining the viability of any liquid-wall MTF scheme. Effects of geometrical convergence, perturbation amplitude and mode, asymmetry of the imploding wave and rotation have thoroughly studied for the case of cylindrical geometry. Typical results are shown in Fig. 3, which emphasises the effect of wave asymmetry on the collapse of initially perturbed cylindrical air cavity.

Fig. 3. Effect of the asymmetry of the imploding wave. Left column shows collapse of the initially perturbed air cavity by perfectly symmetric imploding cylindrical pressure wave. Right column shows collapse of exactly the same cavity when the pressure wave is generated by a single piston (pressure wave arrives from the right).



III. ACOUSTIC DRIVER PROGRESS

The primary component of the acoustic driver consists of a 100 kg, 0.3m diameter hammer piston that is accelerated down a one meter long bore by compressed air. The hammer's position is measured as it traverses the bore and its speed is controlled by an electronic braking system. This control system directs the hammer to impact a stationary anvil piston at a precisely controlled time. The collision generates a large amplitude acoustic pulse that propagates through the anvil and is then transmitted into the liquid metal. A hammer piston of 100 kg driven up to 50m/s will have a kinetic energy of 125 kJ of which approximately 90% is converted into the acoustic wave that propagates toward the target.

To develop this key technology, a series of prototype piston test stands have been built and operated of the course this project. The most advanced full scale test system is HP3b which has fired a total of 850 impacts over the course of the last year, including 39 shots with 50 m/s impact speed. The best high speed timing performance recorded a sequence of 4 consecutive shots, at 50 m/s impact velocity, arrive within 2 μ s of the target time. The steady improvement in the acoustic driver's performance is a result of improved control system signal processing and hammer launching hardware. Work is ongoing to improve the system's shot to shot repeatability. Testing is also progressing to find suitable materials for both the hammer and anvil assemblies. Although the applied loads are similar, the material requirements for the anvils and the hammers are slightly different. The anvils will be in continuous contact with molten metal, so they need to operate at elevated temperatures. Whereas, the hammers don't operate at high temperatures, but they do have complex features machined into them, making them susceptible to failures originating from geometric stress concentrations.

A separate sub-scale test stand called Mini-Piston has been used to test the possible candidates for piston materials (including Bohler-Uddeholm 'Dievar', QuestTek 'Ferrium M54', Carpenter 'AerMet 100', and Vascomax 'C300') for survivability at elevated temperature and high impact velocity. Two samples of small Dievar anvils were subjected to 13 test shots with impact speeds of 50 m/s – 55 m/s. For a given impact speed, the stresses in the small anvils are expected to closely mimic the stresses in the full size anvils. The tests were done at elevated temperature and the anvil faces were in direct contact with molten lead. Although no evidence of cracking was found in these test pieces, significant pitting was observed on the lead interface surface. It is thought that this is likely due to cavitation in the liquid lead.

As a stepping stone toward the a full scale prototype MTF reactor which would employ a synchronized array of over 200 pistons the size of HP3b, a major milestone was completed in 2013 with the commissioning of the Mini-Sphere, (as shown in Fig. 4) a spherical array of 14 full scale piston drivers that synchronously fire into a 1 m diameter spherical volume of liquid lead. The system has a fully functional closed loop

liquid metal pumping system capable of sustaining a stable free-surface vortex cavity in the center of the sphere. The goal of this program is to validate the structural models of the sphere's various components and evaluate the mechanical integrity of the device. Extensive computational fluid dynamics (CFD) and finite element analysis (FEA) numerical testing has been performed to design the Mini-Sphere.

Fig. 4. Mini-Sphere: a 1 meter spherical vessel filled with liquid lead with a synchronized array of 14 full-scale acoustic drivers mounted around the exterior, arranged in two rings of 7 drivers each. The hammers impact anvils that are in direct contact with the liquid lead, imparting pressure pulses into the molten metal. Lead is pumped around the inside of the sphere, creating a cylindrical vortex in the centre of the device. The inner wall of the vortex can then be imaged with fast cameras to record the collapse dynamics.



After the sphere's commissioning was complete, ten shots were made with the full complement of 14 pistons firing under servo control. These shots had impact velocities ranging from 7 m/s to 10 m/s. The resulting vortex collapses were filmed using a high speed camera and the imagery was compared to the results of CFD simulations. In these initial runs it was found that the wall of the vortex turns to a spray soon after the arrival of the pressure wave. This effect is thought to be from a combination of Richtmyer–Meshkov (RM) instabilities on the vortex surface and a poorly formed cavitation region in the lead, generated by pressure pulse reflection very close to the vortex wall. Simulations using the compressible multiphase solver within OpenFOAM CFD software have been conducted that support this interpretation. Work continues to both improve the error in arrival time spread, and to increase the impact velocity. The current goal is to achieve an impact timing error spread of $\pm 10\mu\text{s}$ with an impact speed of 20 m/s. Work also continues to understand and control the spray that is generated during the collapse of the vortex. CFD models of the geometry of the pressure wavefront propagation show that due to the small size of the Mini-Sphere, the pressure field from the 14 pistons is expected to generate an inward displacement of the vortex surface that is initially larger at the center and smaller toward the poles of the sphere. With the compression surface forming a hyperboloid instead

of the desired ellipsoid, the RM instability is likely enhanced rather than suppressed.

IV. PROGRESS ON SELF-CONFINED PLASMAS

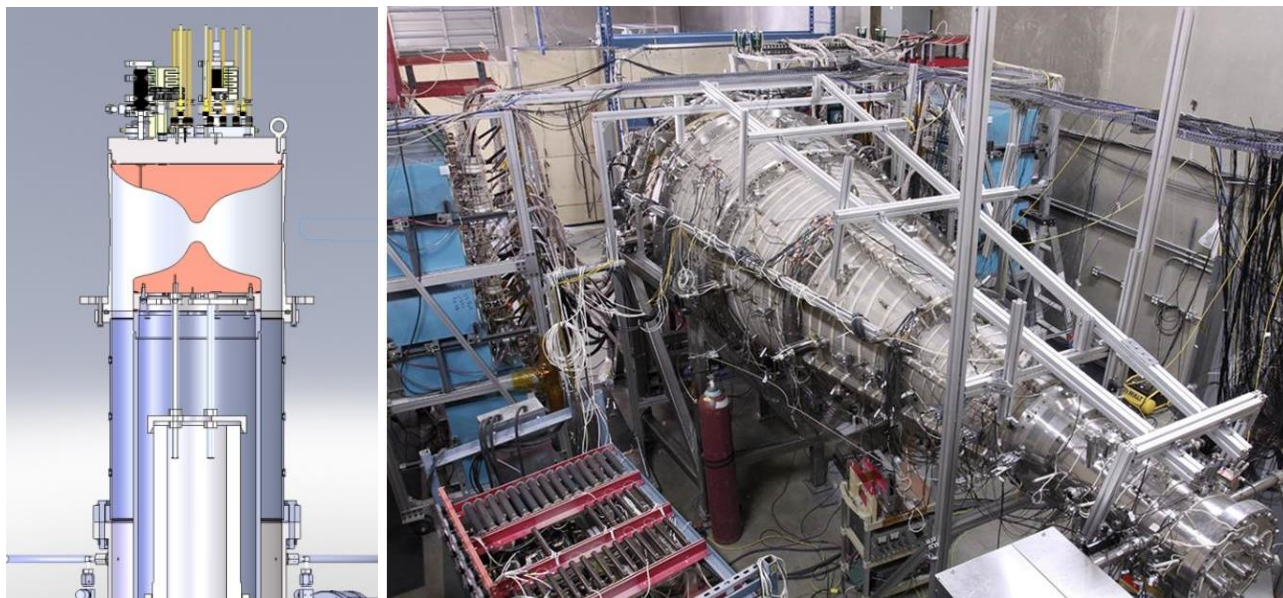
General Fusion is currently operating two types of plasma devices, a small direct formation device named the Magnetized Ring Test (MRT) as well as set of larger and more energetic conical compression devices known as Plasma Injectors (PI-1 and PI-2). Both types of devices employ a magnetized Marshall gun to form spheromak plasma configurations. A schematic of MRT is shown in Fig. 5 (a) and PI-1 is pictured in Fig. 5 (b). Both PI-1 and PI-2 have the same overall electrode geometry. They are 5 meters long and 1.9 m in diameter at the expansion region where a high-aspect ratio spheromak ($R_{\text{major}}/r_{\text{minor}} = 4.4$) is formed with a minimum λ of 9 m^{-1} . The acceleration stage is 4 m long and tapers to an outer diameter of 40 cm. The capacitor banks store 0.5 MJ for formation and 1.13 MJ for acceleration. Power is delivered via 62 independently controlled switch modules. Several geometries for formation bias field, inner electrodes and target chamber have been tested, and trends in accelerator efficiency and target lifetime have been observed. Thomson scattering and ion Doppler spectroscopy show significant heating ($>200\text{ eV}$) as the CT is compressed in the conical accelerator. B-dot probes show magnetic field structure consistent with Grad-Shafranov models and MHD simulations, and CT axial length depends strongly on the λ profile.

The compact toroids generated by these systems are a self-organized spheromak configurations containing embedded toroidal and poloidal magnetic fields and corresponding plasma currents, which decay dominantly by resistive dissipation of the plasma currents over several hundred microseconds. The acceleration stage of the plasma injectors act to fill the region behind the CT with an unbalanced toroidal flux, created by an externally applied railgun current that passes radially across the back side of the CT. The magnetic pressure from this toroidal pushing field acts to accelerate the CT to speeds in excess of 100 km/s, and provides the force to compress it into the conical self-similar converging electrodes to a radial 4x compression ratio, thereby boosting the magnetic field, density and temperature. In the MTF reactor design the pair of plasma injectors would be positioned at either end of the liquid metal vortex cavity, and the relative helicities of the CTs would be such to enable reconnective merging in the center of the vortex cavity. This merging would provide a near-zero final momentum for the target plasma to enable the capture by the compression wave. However the option of a single CT, non-merged target plasma is also being considered, and may have practical advantages if it proves possible to create fusion-relevant plasma conditions via that route.

Careful investigation of the parameter space of plasma injector operation coupled with improvements in computer simulation has resulted in a significant improvement in the heat confinement during the CT formation and pre-

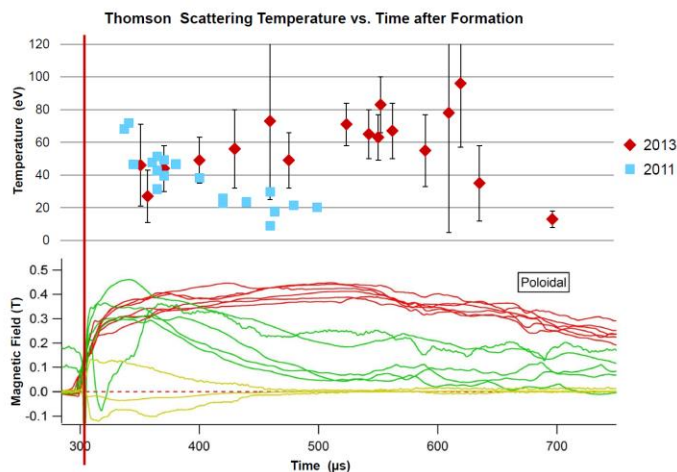
acceleration phase on PI-1. Confinement improved to the point that compressional heating via contraction of the CT and/or Ohmic heating of the plasma was observed during formation. This result is shown in Fig. 6. Heating continued for ~200 microseconds until the magnetic surfaces crossed through an instability resulting in distortions in the flux surfaces and loss of confinement.

Fig. 5. (a) Magnetized Ring Test (MRT) on left, (b) Plasma Injector-1, right.



Advances from simulation of the plasma dynamics has made use of both faster running 2-D (axially symmetric) as well of 3-D simulations to reveal behavior that cannot be captured by 2-D simulations. Simulation predicted a large improvement in CT symmetry by the addition of a toroidal bias field and this prediction was subsequently experimentally confirmed. Our primary simulation tool is the Versatile Advection Code (VAC), which is a shock-capturing magnetohydrodynamics (MHD) code.

Fig. 6. Comparison of early (2011) and recent (2013) T_e measurements as a function of time during a formation-only PI-1 discharge. Poloidal B at several different axial positions is shown in the lower graph for a 2013 discharge.



The General Fusion version of VAC has been augmented to include coupling to lumped circuits (the formation and acceleration capacitor banks) and additional physics such as radiative cooling, plasma viscosity, etc. As well as improving the main simulation code itself, we also introduced more powerful techniques for analyzing simulation results, such as the safety factor profile, mode structure, and magnetic surface stochasticity (Fig. 7). In addition we have recently begun using the fusion-community CORSICA code for generation of

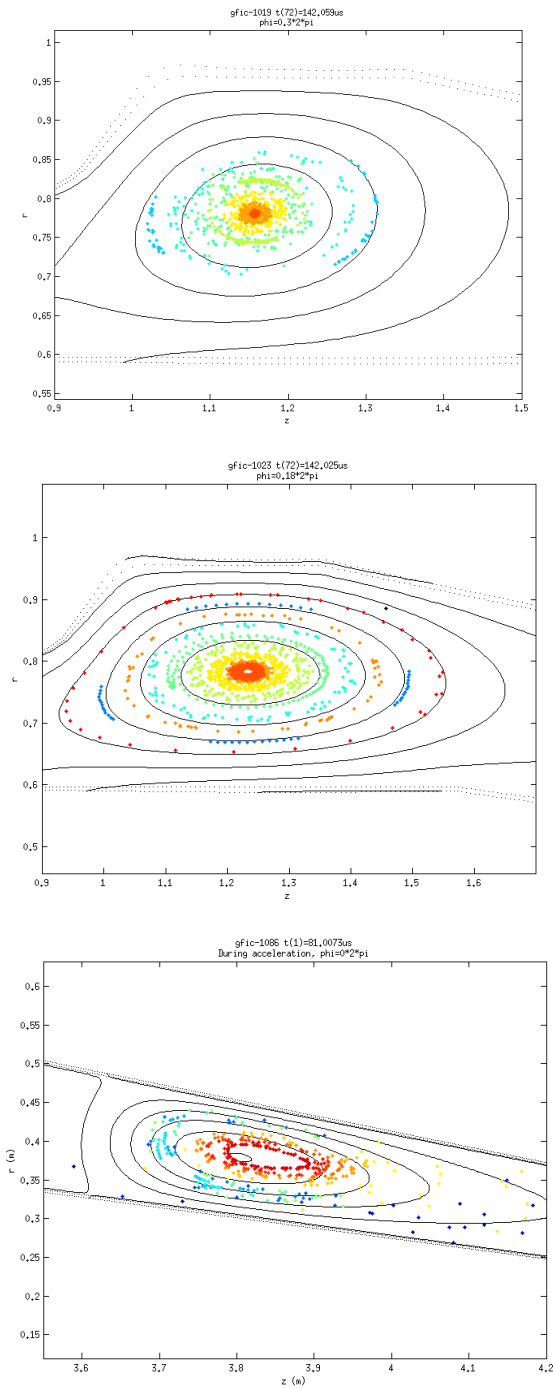
plasma equilibria for simulation as well as for fitting of experimental data.

Subsequent acceleration of the well-formed CT indicated adiabatic heating of the CT. A compact toroid formed at location $z = 1.18$ m with $B_p = 0.2$ T, $T_e = 40$ eV, and $n_e = 0.5 \times 10^{20} \text{ m}^{-3}$ when accelerated had $B_p = 0.8$ T, $T_e = 160$ eV, $n_e = 4 \times 10^{20} \text{ m}^{-3}$ when its core passed the $z = 3.52$ m location (2x radial compression), which is consistent with adiabatic compressional heating likely only possible with non-stochastic closed flux surfaces and negligible radiation losses. However when further compressed to the $z = 4.93$ m location (total 4x radial compression) there was still approximate conservation of poloidal flux with $B_p = 3.0$ T, and expected density increase to $n_e = 3 \times 10^{21} \text{ m}^{-3}$ yet Thomson scattering measurements of electron temperature yielded only $T_e = 250$ eV, far below adiabatic expectations. Presently it is unclear what loss mechanism is responsible for this. Increase of emission in the visible, VUV and soft X-rays are observed during this period, however, enhanced transport due to magnetic fluctuations is also not yet ruled out.

In contrast to the larger PI-1,2 injectors, the smaller MRT device does away with the acceleration/pre-compression stage and attempts to form a high flux CT directly within an implodable cylindrical liner composed of aluminum. The MRT electrodes form a bow-tie geometry known for its high beta stability. Unlike PI-1,2 it is not designed to be a prototype

component of the ultimate MTF reactor, but rather as an independent plasma compression experiment where a sequence of implosive compression tests can be conducted to observe the behavior of a high density magnetized plasma as it experiences increasing beta, possible interactions with the liner wall, and shifting of magnetic geometries as the compression proceeds.

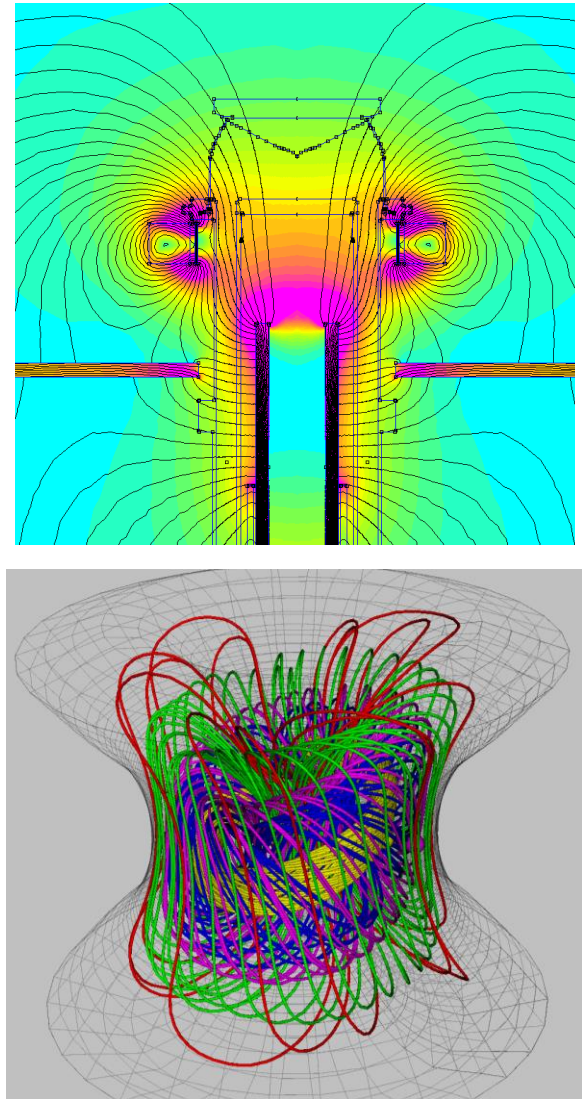
Fig. 7. Puncture plots of the magnetic field from 3-D VAC simulations of the PI-1 device. Top: standard spheromak formation. Middle: formation with toroidal bias field. Bottom: CT during acceleration at $z = 3.7$ m. Black contours show toroidally averaged Ψ (poloidal flux) surfaces.



The primary work so far with MRT has been formation-only discharges to determine the intrinsic initial plasma behavior of the bow-tie spheromak without any additional compression. This is leading up to full implosion tests where plasma temperatures may reach significant D-D fusion cross sections if the compression can proceed near adiabatically. To date the MRT system in formation-only mode has reached sustained electron temperatures of 75 eV and overall lifetime of over 100 μ s when operating with deuterium.

In the MRT work we introduced the use of a finite-element code (FEMM) to calculate magnetic field profiles in the presence of iron components (Fig. 8a). These profiles are part of the initial conditions required to begin a 3-D MHD simulation of the tilt instability that may occur during compression by a central pinch deformation of the aluminum liner (Fig. 8b).

Fig. 8. (a) MRT poloidal bias magnetic field, (b) 3-D B-field structure undergoing tilt mode during a liner compression simulation.



V. NEAR-TERM FUTURE PLANS

A high priority in the near-term objectives is the development of higher efficiency plasma injector devices that can robustly operate at high power. While the results so far have been promising, the path to practical MTF would greatly benefit from improvements in efficiency and finesse of the operation of the plasma injectors that are responsible for creating robustly stable target plasmas. One possible avenue for improvement includes exploration of non-conical injector designs such as a so-called “trumpet” design, which has been simulated and shows promise.

Overall the task of benchmarking simulation to experimental results to improve their predictive ability will remain a high priority during the current phase of the project. Simulation for use as a design optimization tool will hopefully aid in finalizing the design details of a the first full-scale prototype reactor (operating at low rep-rate) and proceeding forward with the implementation.

VI. SUMMARY

The previous year has seen much progress towards creating and compressing plasma and the outlook is now very encouraging. In particular, plasma densities of 10^{20} ions/m³ at >250 eV electron temperatures and up to 500 eV plasma ion temperatures have been demonstrated. Indications are that the formation region of the injector has achieved closed flux surfaces and that these surfaces are maintained during acceleration allowing for adiabatic compression and heating. Piston impact speeds of 50 m/s and servo-controlled impact timing accurate to $\pm 2 \mu\text{s}$ have been achieved. The 14-piston liquid Pb Mini-Sphere assembly for testing vortex generation and piston impact has been fully commissioned and is collecting data.

General Fusion has continued to make progress in forming and accelerating compact toroids (CT) and is nearing the requirements for long lasting, stable, and hot CTs in the target chamber. A series of design changes were implemented and tested, eventually resulting in good formation and acceleration of CTs. The acceleration current now delivers most of its energy into acceleration, allowing it to reach elevated

temperatures and magnetic fields. Formation efficiency is ~45% and acceleration efficiency is ~20% (energy in CT/discharge energy from relevant capacitor bank).

General Fusion has gained momentum by recent progress on all fronts of the MTF program. Improvements in piston survival, liquid Pb handling, plasma temperature, acceleration efficiency, injector reliability, and regulatory matters have left the team and investors with a positive outlook on the coming year and the company’s ability to meet goals.

ACKNOWLEDGMENT

The authors would like to acknowledge the work of the entire General Fusion team for their ongoing efforts in the development of this technology. General Fusion is funded by private investors including Chrysalix Energy Ventures, Growthworks, Business Development Bank of Canada, Braemar Energy Ventures, Entrepreneurs Fund, SET Ventures, Bezos Expeditions, and Cenovus Energy. General Fusion’s work is also funded in part by a grant from Sustainable Development Technology Canada.

REFERENCES

- [1] J. D. Lawson, “Some Criteria for a Power Producing Thermonuclear Reactor”, Proceedings of the Physical Society. Section B, Vol. 70, Iss. 1, 1957.
- [2] R. L. Miller and R. A. Krakowski, “Assessment of the slowly-imploding liner (LINUS) fusion reactor concept”, 4th ANS Topical Meeting on the Technology of Controlled Nuclear Fusion, 1980 October 14-17.
- [3] R. Siemon, I Lindemuth, K. Schoenberg, “Why Magnetized Target Fusion Offers A Low-Cost Development Path for Fusion Energy”, Comments on Plasma Physics and Controlled Fusion, 1997.
- [4] R. Siemon et al., “The relevance of Magnetized Target Fusion (MTF) to practical energy production, a white paper for the Fusion Energy Sciences Advisory Committee”, Los Alamos National Labs, 1999, http://fusionenergy.lanl.gov/Documents/MTF/MTF_Appl._whitepaper_6-99.PDF
- [5] D. Dudzick, “Nucleonic aspects of the LINUS imploding blanket”, ANS Meeting on the Technology of Controlled Thermonuclear Fusion, Santa Fe, New Mexico, USA, 1978 May 9.
- [6] M. E. Sawan, M. A. Abdou, “Physics and technology conditions for attaining tritium self-sufficiency for the DT fuel cycle”, Fusion Engineering and Design, Vol. 81, 2006, pp. 1131-1144.
- [7] M. Moyer, “Fusion’s False Dawn”, Scientific American, March, 2010, pp. 50-57.